

# PREDICTION OF CRITICAL STRESS AND STRAIN FOR THE ONSET OF DYNAMIC RECRYSTALLIZATION IN PLAIN CARBON STEELS

M. Shaban Ghazani<sup>\*1</sup>, A. Vajd<sup>2</sup> and B. Mosadeg<sup>2</sup>

\* Mehdi.mse@gmail.com

Received: June 2014

Accepted: December 2014

<sup>1</sup> Young Researchers and Elite Club, Ilkhchi Branch, Islamic Azad University, Ilkhchi, Iran.

<sup>2</sup> Technical College of Tabriz No.2, Technical and Vocational University, Tabriz, Iran.

**Abstract:** The aim of the present study is the prediction of critical conditions (including critical strain and flow stress) for the initiation of dynamic recrystallization during thermo-mechanical processing of plain carbon steels. For this propose, torsion tests were conducted at different temperature (1050, 1100 and 1150°C) and strain rates (0.002, 0.02 and 0.2/s). All flow curves showed a peak stress indicating that dynamic recrystallization occurs during hot deformation. The critical stress and strain were then determined based on change in strain hardening rate as a function of flow stress. Finally, the effect of deformation conditions on these parameters was analyzed.

**Keywords:** Dynamic recrystallization, Critical stress, Critical strain, Low carbon steel.

## 1. INTRODUCTION

When materials with high stacking fault energy are deformed at high temperatures, the increase in dislocation density (and thus flow stress) associated with work hardening is compensated by the annihilation or rearrangement of dislocations into lower-energy substructures. This process is termed dynamic recovery. The annihilation rate of dislocations increases with the dislocation density, which eventually reaches equilibrium with the generation of new dislocations by continued deformation, resulting in steady-state flow. By contrast, in metals with lower stacking fault energy, the ability of dislocations to climb and/or cross-slip is hindered. This results in a denser and less homogeneous dislocation distribution. Local dislocation densities eventually reach levels high enough to favor the nucleation of new grains. The growth of these softer grains eventually results in measurable changes in the overall mechanical behavior of the material, in particular one or more peaks in the flow stress. This process is termed dynamic recrystallization (DRX), and has been shown to occur in austenite phase in steels over a wide range of conditions [1-2]. The peak in the stress-strain curve is the major mechanical indication for the occurrence of DRX [3-5]. The strain at the start of recrystallization (the critical

strain,  $\epsilon_c$ ) is actually slightly lower than the peak strain ( $\epsilon_p$ ) because the peak strain is due to the work hardening being exactly offset by dynamic recrystallization [6]. In other words, the strength decreases only when the level of dynamic recrystallization is sufficient to counter the work hardening. In the case of austenitic steels, this critical strain for the onset of dynamic recrystallization can be determined by direct observation of microstructure after hot deformation [7- 8]. However when plain low carbon or micro-alloyed steels are subjected to hot deformation, the  $\gamma \rightarrow \alpha$ +perlite transformation occurs during cooling after deformation and austenite phase can't be directly observed at ambient temperature [9]. In this case an alternative method developed by Ryan [10] is used to indirect determination of critical strain for the onset of dynamic recrystallization. In this method the critical strain is defined as the strain at which the experimental flow curve deviates from dynamic recovery behavior, based on difference in the strain hardening associated with dynamic recrystallization and recovery. Thus the critical stress is identified by the inflection point in the  $\theta$ - $\sigma$  curve (where  $\theta=d\sigma/d\epsilon$ ) [11].

The present work aims to investigate dynamic recrystallization event in plain low carbon steel. A study has been carried out to determine critical conditions (strain and flow stress) for the onset of

dynamic recrystallization. The effect of deformation conditions on critical stress and strain was also investigated.

## 2. MATERIAL AND EXPERIMENTAL PROCEDURE

The material used in this study is a plain low carbon steel of the chemical composition shown in table 1. The steel was prepared as 30 kg ingot in an induction furnace operating under argon atmosphere, and then refined by electro-slag remelting (ESR) in a laboratory unit. The ingot was reheated to 1200°C for 1 h and hot rolled in six passes to 25 mm thick plate. Torsion samples with a gauge of 20mm length and 6.7mm diameter were machined out from plates with the longitudinal axis parallel to the rolling direction. Hot torsion tests were conducted at different temperature (1050, 1100 and 1150°C) and strain rates (0.002, 0.02 and 0.2/s). The deformation procedure for the study of dynamic recrystallization involved preheating at 1200°C for 180s followed by cooling to deformation

temperature at the rate of 1°C/s. For temperature homogenization purposes, samples were held for 3min prior to deformation. All samples were deformed to strains up to 0.6. The utilized deformation schedule is shown in Fig. 1.

## 3. RESULTS AND DISCUSSION

### 3.1. Hot Flow Curves

Flow curves obtained for plain carbon steel deformed at different temperature and strain rates are shown in Fig. 2. As can be seen the obvious peak stress in these curves indicates the occurrence of dynamic recrystallization. In addition, the peak stress and strain is increases with increasing strain rate at the constant deformation temperature.

### 3.2. Deformation Activation Energy

So far, various empirical equations have been proposed to quantify hot deformation characteristics of steels. The most frequently used one is as follows [12]:

$$\sigma_{ss} = A \left[ \dot{\epsilon} \exp\left(\frac{Q_d}{RT}\right) \right]^q \quad (1)$$

**Table 1.** Chemical Composition of plain carbon steel (Wt.%)

C	Si	Mn	S	P	Al	N	Fe
0.14	0.22	1.8	0.004	0.015	0.02	0.002	bal

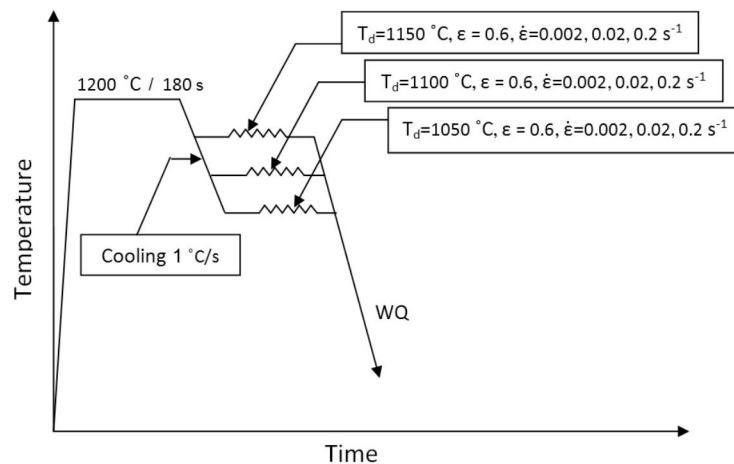


**Fig.1.** Hot Deformation schedule for the study of dynamic recrystallization behavior of plain carbon steel.



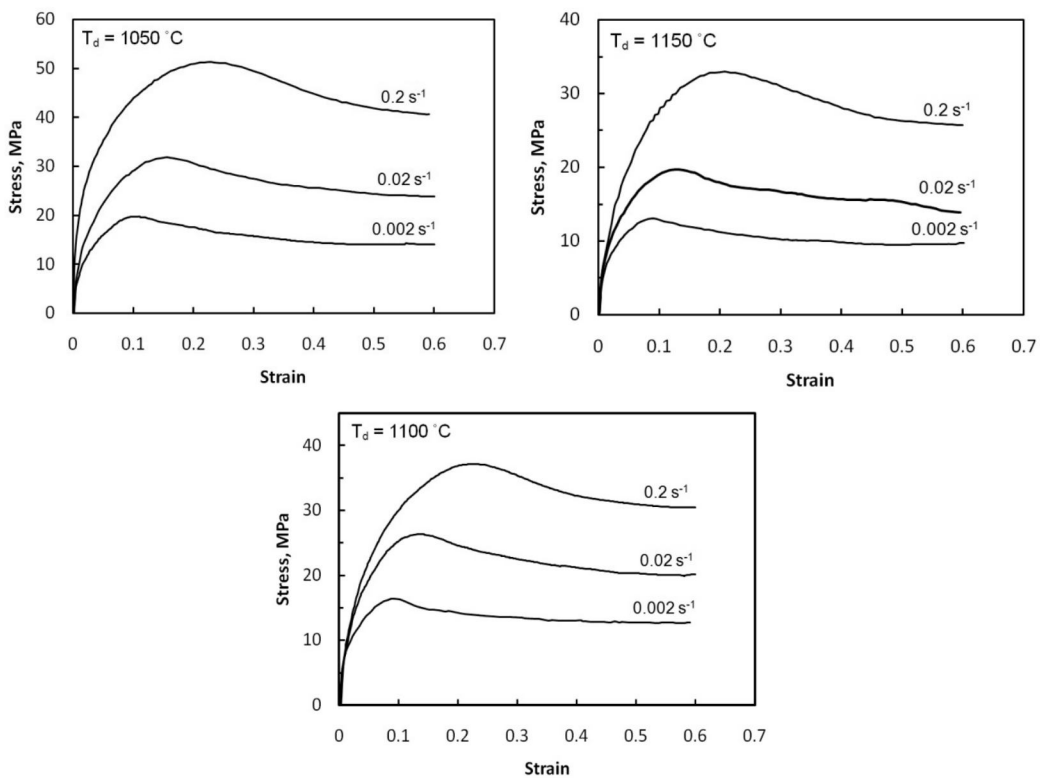


Fig.2. Typical hot flow curves of plain carbon steel deformed at different temperature and strain rates.

Where  $\sigma_{ss}$  is steady state stress, A is a constant depending on the chemical composition and initial austenite grain size,  $\dot{\epsilon}$  is strain rate,  $Q_d$  is activation energy for plastic deformation, R is gas constant, T is temperature and q is the power low exponent. As shown in Fig. 3, the value of power low exponent is determined from the slope of the

plot of the steady state stress as a function of strain rate at constant temperature. This value is calculated as 0.22 for this investigated carbon steel. Fig. 4 shows the effect of temperature on steady state stress at constant strain rate. The slope of the plot of steady state stress as a function of inverse temperature at constant strain

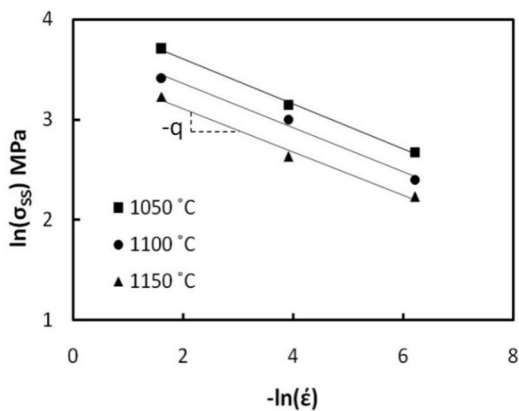


Fig.3. Effect of strain rate on the steady state stress at constant temperature.

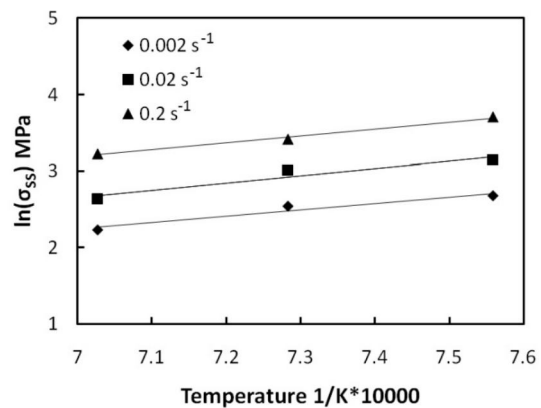


Fig.4. Effect of temperature on the steady state stress at constant strain rate.

rate is equal to  $q^*Q_d/R$ . Therefore, the activation energy for plastic deformation of austenite was calculated as 335 KJ/mol.

### 3. 3. Critical Stress and Strain

The critical stress and strain for initiation of DRX can be calculated from hot flow curves based on difference between work hardening characteristics of DRX and DRV. As shown in Fig. 5, the method proposed by Ryan and McQueen defines the critical stress as the stress at the inflection point of  $\theta$ - $\sigma$  plot (where  $\theta$  is  $d\sigma/d\varepsilon$ ).

To determine the inflection point of  $\theta$ - $\sigma$  plot, it's necessary to find an equation that best fits the experimental  $\theta$ - $\sigma$  data from zero to peak stress. The simple equation is third order equation:

$$\theta = \left(\frac{\partial\sigma}{\partial\varepsilon}\right)_\varepsilon = A\sigma^3 + B\sigma^2 + C\sigma + D \quad (2)$$

$$\frac{d\theta}{d\sigma} = A\sigma^2 + 2B\sigma + Cn \rightarrow \frac{d^2\theta}{d\sigma^2} = 6A\sigma + 2B = 0$$

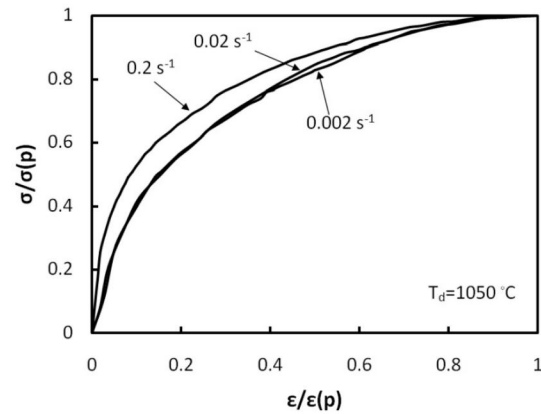


Fig.6. Normalized flow curves of carbon steel deformed with different strain rates at 1050°C.

To calculate the critical stress for the onset of DRX the normalized flow curves ( $\sigma/\sigma_p$ - $\varepsilon/\varepsilon_p$ ) were obtained from zero to peak strain. Fig. 6 shows the normalized flow curves of steel deformed at 1050 °C at different strain rates. The corresponding normalized strain hardening versus stress curves are shown in Fig. 7. The first order derivative of strain hardening rate as a function of stress is also represented in this

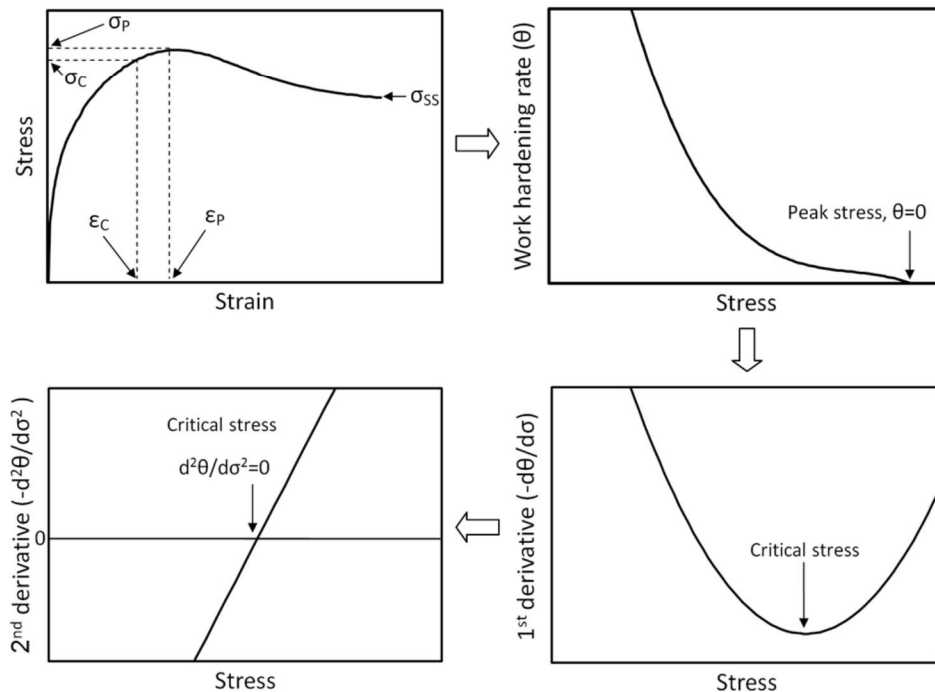


Fig. 5. The procedure for determination of critical stress for the onset of DRX.

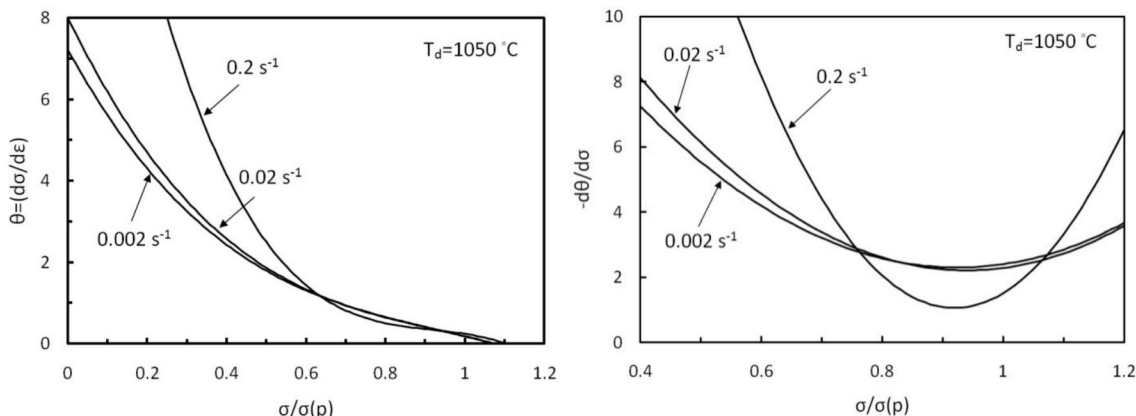


Fig.7.  $\theta$ - $\sigma$ N and  $(d\theta/d\sigma)$ -  $\sigma$ N plots of carbon steel deformed with different strain rates at 1050°C.

Table 2.  $\theta$ - $\sigma$  equations and obtained critical stress and strains at different deformation conditions.

Strain rate ( $s^{-1}$ )	T( $^{\circ}C$ )	$\theta$ - $\sigma^N$ relation	$\sigma_c$ (MPa)	$\epsilon_c$	
0.002	1050	$\theta = -6\sigma^3 + 16.65\sigma^2 - 17.68\sigma + 7.22$	0.92	19.20	0.071
	1100	$\theta = -17.98\sigma^3 + 45.18\sigma^2 - 39.84\sigma + 12.8$	0.83	13.68	0.057
	1150	$\theta = -9.32\sigma^3 + 25.11\sigma^2 - 24.63\sigma + 9.03$	0.89	10.81	0.055
0.02	1050	$\theta = -6.75\sigma^3 + 19.06\sigma^2 - 20.13\sigma + 8.014$	0.93	29.93	0.110
	1100	$\theta = -7.06\sigma^3 + 18.6\sigma^2 - 18.34\sigma + 7.01$	0.87	22.95	0.076
	1150	$\theta = -16.88\sigma^3 + 46\sigma^2 - 42.69\sigma + 13.85$	0.90	17.88	0.073
0.2	1050	$\theta = -23.1\sigma^3 + 64.03\sigma^2 - 59.94\sigma + 19.36$	0.91	46.22	0.138
	1100	$\theta = -6.4\sigma^3 + 17.37\sigma^2 - 17.92\sigma + 7.20$	0.89	34.04	0.133
	1150	$\theta = -4.66\sigma^3 + 12.81\sigma^2 - 14.589\sigma + 6.62$	0.91	30.18	0.126

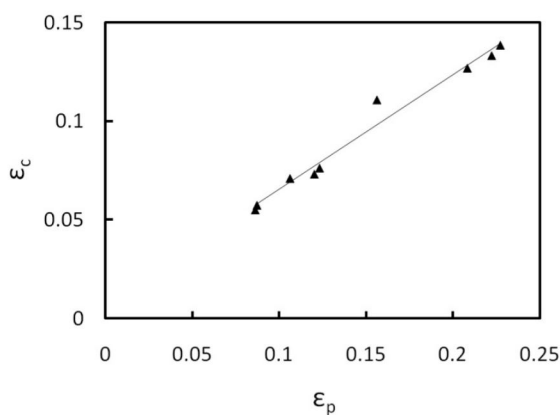


Fig. 8. Relationship between critical and peak strains at different temperature and strain rates.

figure. All calculated  $\theta$ - $\sigma$  equations and obtained

critical stress and strains for the onset of DRX at different temperature and strain rates are represented in Table. 2.

Fig. 8 shows the relation between critical and peak strains. The critical strain for the onset of DRX has been found to be a constant fraction of peak strain ( $\epsilon_c = 0.59 \epsilon_p$ ). This value is in the range of those reported for carbon steels with coefficients from 0.4 to 0.85[10-13]. Dependence of critical stress for initiation of DRX to Zener-Hollomon parameter is represented in Fig. 9. The relationship between normalized critical stress ( $\sigma_c/\sigma_p$ ) and Z parameter is also shown in this figure. As can be seen there is a linear relationship between  $\sigma_c$  and Z perimeter as follows:

$$\sigma_c(\text{Mpa}) = 4.9 \ln(Z) - 99.47 \quad (3)$$



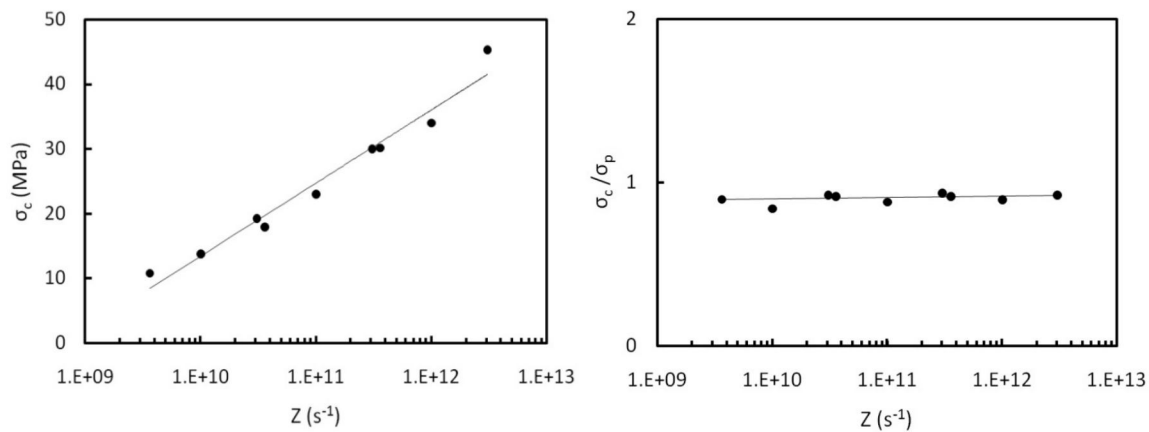


Fig. 9. Relationship between critical stress for the onset of DRX and Zener-Hollomon parameter.

Although the critical stress is dependent on deformation conditions, the normalized critical stress for the onset of DRX is almost constant and there is a lack of dependence on deformation conditions ( $\sigma_c/\sigma_p=0.9$ ).

#### 4. CONCLUSIONS

1. The method proposed by Ryan and McQueen to calculate critical strain and flow stress for the onset of DRX was described briefly.
2. It was found that there is a linear relationship between critical stress and logarithm of Zener-Hollomon parameter.
3. The normalized critical stress is independent on deformation conditions and for 0.14%C-1.8%Mn steel the value of  $\sigma_c/\sigma_p$  is approximately about 0.9.
4. The critical strain for the onset of DRX is a constant fraction of peak strain and for 0.14%C-1.8%Mn steel, this constant is about 0.59.

#### REFERENCES

1. Barraclough, D. R., "Hot working and recrystallization of a stainless and a low alloy steel", Ph. D. Thesis, University of Sheffield, Sheffield, UK, 1974.
2. Barraclough, D. R., Sellars, C. M., "Static

recrystallization and restoration after hot deformation of type 304 stainless steel", *Met. Sci*, 1979, 13, 257-267.

3. Sakai, T., Jonas, J. J., "Dynamic recrystallization: mechanical and microstructural considerations", *Acta Metallurgica*, 1984, 32, 189-209.
4. Busso, E. P., "A continuum theory for dynamic recrystallization with microstructure-related length scales", *Int. J. Plast.*, 1998, 14, 319-353.
5. Ding, R., Guo, Z. X., "Coupled quantitative simulation of microstructural evolution and plastic flow during dynamic recrystallization", *Acta Materialia*, 2001, 49, 3163-3175.
6. Poliak, E. I., Jonas, J. J., "Initiation of dynamic recrystallization in constant strain rate hot deformation", *ISIJ Int*, 2003, 43, 684-691.
7. Salvatoti, I., Inoue, T., Nagal, K., "Ultrafine grain structure through dynamic recrystallization for type 304 stainless steel", *ISIJ Int*, 2002, 42, 744-750.
8. Stewart, G. R., Jonas, J. J., Montheillet, F., "Kinetics and critical conditions for the initiation of dynamic recrystallization in 304 stainless steel", *ISIJ Int*, 2004, 44, 1581-1589.
9. Cho, S. H., Kang, K. B., Jonas, J. J., "The dynamic, static and metadynamic recrystallization of Nb-microalloyed steel", *ISIJ Int*, 2001, 41, 63-69.
10. Ryan, N. D., McQueen, H. J., "Dynamic softening mechanisms in 304 austenitic stainless steel", *Can. Met. Q.*, 1990, 29, 147-162.

11. Sun, X., Luo., H., Dong, H., Liu, Q., Weng, Y., “Microstructural evolution and kinetics for post-dynamic transformation in a plain low carbon steel“, *ISIJ Int*, 2008, 48, 994-1000.
12. Sellars, C. M., Davies, G. J., “Hot working and forming processes”, *Proceeding of the international conference on Hot Working and Forming Processes*, Metals Society, London, 1980.
13. Kiriata, A., Siciliano, F., Maccagno, T. M., Jonas, J. J., “Mathematical modeling of mean flow stress during the hot strip rolling of multiply-alloyed medium carbon steels“, 1998, *ISIJ Int*, 38, 187-195.